

**MULTIPLE LINEAR REGRESSION MODELS  
FOR ESTIMATING TRUE SUBSURFACE  
RESISTIVITY FROM APPARENT RESISTIVITY  
MEASUREMENTS**

**MUHAMMAD SABIU BALA**

**UNIVERSITI SAINS MALAYSIA**

**2018**

**MULTIPLE LINEAR REGRESSION MODELS  
FOR ESTIMATING TRUE SUBSURFACE  
RESISTIVITY FROM APPARENT RESISTIVITY  
MEASUREMENTS**

by

**MUHAMMAD SABIU BALA**

**Thesis submitted in fulfillment of the requirements  
for the degree of  
Doctor of Philosophy**

**June 2018**

## ACKNOWLEDGEMENT

All thanks, praises and total glorifications are due to Allah (S.W.T.), the Lord of mankind and the Sustainer of the universe. May His peace and blessings be upon His Noble Prophet, Muhammad (S.A.W), his household and his companions. This research work is not a solo endeavour; many people have contributed to it in many ways. The greatest contribution came from my major supervisor, Associate Professor Dr. Rosli Saad, who has offered uncommon intellectual guidance, tireless encouragement and extraordinary inspiration to take me through this work, from its conception to its completion. No words can ever describe how much he has done. It is indeed a rare privilege to have such a formidable supervisor giving you exceptionally brilliant guidance on each step you take. I will remain eternally grateful to him. Dr. Nordiana Mohd Muztaza, Dr. Nur Azwin Ismail, Dr. Andy Anderson Berry, Mr. Yaakob Othman and the rest of Geophysics staff too have provided so much insightful appraisals and invaluable advice and constant encouragement, I find it very difficult to thank them enough.

For financial and other forms of aid needed for the success of this study, my profound appreciation goes to my supervisor, Associate Professor Dr. Rosli Saad and Dato' Prof. Mokhtar Saidin, Director of Centre for Global and Archaeological Research, Universiti Sains Malaysia. For other contributions, ranging from offering useful advice and doing paperwork to data acquisition, learning software applications and construction of the new resistivity estimation template, my warm gratitude goes to Rais Yusoh, also a PhD student under the same supervisor. I would also like to thank my friends and lab mates, Sabrian Tri Anda, Fauzi Andika, Amsir Taib, Kiu Yap Chong, Mark Jinmin, Nazrin Rahman, Mohd Hazreek Zainal Abidin, Mustafa

Muhammad Adejo and Najmiah Rosli, all postgraduate students of Geophysics, USM. I would like to particularly thank all my friends, Dr. Mukhtar Abubakar Balarabe, Dr. Yakubu Mingyi Samuel, Nuraddeen Usman and many teeming certified Nigerian students at USM for their participation in this study and all those who contributed to its success in whatever form.

Finally, I express my heartfelt gratitude to my late parents Muhammad Ashiru and Amina Muhammad, to my late grandfather Alhaji Bala Yandaka, to my wife Bilkisu, to my son Ahmad, to all my siblings especially Saadatu, Bilkisu and Amina, to my uncles Abdulkadir and Kabir for their unfailing support, love and encouragement at every stage of my pursuit.

This work is dedicated Allah, the Most Beneficent the Most Merciful, by Whose grace I become what I am today despite my weaknesses.

## TABLE OF CONTENTS

Acknowledgement	ii
Table of Contents	iv
List of Tables	vii
List of Figures	ix
List of Symbols	xiii
List of Abbreviations	xiv
Abstrak	xv
Abstract	xvii
<b>CHAPTER 1: INTRODUCTION</b>	<b>1</b>
1.0 Background	1
1.1 Problem statements	3
1.2 Research objectives	4
1.3 Scope of the study	5
1.4 Research significance and novelty	6
1.5 Thesis layout	7
<b>CHAPTER 2: LITERATURE REVIEW</b>	<b>9</b>
2.0 Introduction	9
2.1 Fundamentals of resistivity method	9
2.2 Four electrodes method for measuring subsurface resistivity	14
2.2.1 Wenner array	16
2.2.2 Wenner-Schlumberger array	17
2.2.3 Dipole-dipole array	18
2.3 Inversion of resistivity data	19

2.4	Previous works	20
2.5	Chapter summary	42
<b>CHAPTER 3: RESEARCH METHODOLOGY</b>		<b>44</b>
3.0	Introduction	44
3.1	Overall work plan for the study	44
3.2	Linear regression method	47
3.3	Resistivity data	48
3.4	Models' calibration	50
3.4.1	Study area	51
3.4.2	Selection of variables and diagnostic checks	53
3.4.3	Development of linear regression models	55
3.5	Models' accuracy assessment	57
3.5.1	Coefficient of determination ( $R^2$ )	58
3.5.2	Adjusted coefficient of determination ( $R^2_{adj}$ )	59
3.5.3	Root-mean-square error ( $RMSE$ )	59
3.5.4	Weighted mean absolute percentage error ( $wMAPE$ )	60
3.6	Models' validation	60
3.6.1	Site A – USM main campus, Pulau Pinang, Malaysia	62
3.6.2	Site B – Sungai Batu, Pulau Pinang, Malaysia	63
3.6.3	Site C – USM Engineering Campus, Penang, Malaysia	65
3.6.4	Site D – Lembah Bujang, Kedah, Malaysia	67
3.6.5	Site E – Kampung Ulu Slim, Perak, Malaysia	68
3.6.6	Site F – Pulo, Seulimeum, Aceh Besar, Indonesia	70
3.6.7	Site G – Tongod, Linayukan, Sabah, Borneo Island	72
3.6.8	Site H – University of Lagos campus, Nigeria	75
3.7	Comparison models' performance with other establishes techniques	77

3.8	Chapter summary	78
<b>CHAPTER 4: RESULTS AND DISCUSSION</b>		<b>79</b>
4.0	Introduction	79
4.1	Linear regression's basic assumptions diagnostics	79
4.2	Linear regression models result	84
4.3	Numerical (accuracy) assessments of the generated models	86
4.4	Models' validation at test sites	95
4.4.1	Site A – USM main campus, Pulau Pinang, Malaysia	95
4.4.2	Site B – Sungai Batu, Pulau Pinang, Malaysia	102
4.4.3	Site C – USM Engineering Campus, Penang, Malaysia	103
4.4.4	Site D – Lembah Bujang, Kedah, Malaysia	110
4.4.5	Site E – Kampung Ulu Slim, Perak, Malaysia	114
4.4.6	Site F – Pulo, Seulimeum, Aceh Besar, Indonesia	117
4.4.7	Site G – Tongod, Linayukan, Sabah, Borneo Island	118
4.4.8	Site H – University of Lagos campus, Nigeria	120
4.5	Models' performance in comparison with established techniques	122
4.6	True resistivity estimation templet	123
4.7	Chapter summary	126
<b>CHAPTER 5: CONCLUSIONS AND RECOMMENDATIONS</b>		<b>127</b>
5.0	Conclusions	127
5.1	Recommendations	129
<b>REFERENCES</b>		<b>130</b>
<b>APPENDICES</b>		
<b>LIST OF PUBLICATIONS</b>		

## LIST OF TABLES

		<b>Page</b>
Table 2.1	Resistivity of some common rocks and soil materials (Reynolds, 1997; Lowrie, 2007)	10
Table 3.1	Hierarchical combination of independent variables	55
Table 4.1	Normality test of the dependent variable using statistical descriptives	80
Table 4.2	Models with generated coefficients for Wenner array	85
Table 4.3	Models with generated coefficients for Wenner-Schlumberger array	85
Table 4.4	Models with generated coefficients for Dipole-dipole array	86
Table 4.5	Numerical assessment of overall linear regression models calibrated for Wenner array	89
Table 4.6	Numerical assessment of overall linear regression models calibrated for Wenner-Schlumberger array	91
Table 4.7	Numerical assessment of overall linear regression models calibrated for Dipole-dipole array	93
Table 4.8	Errors occurred on testing the overall regression models for the three arrays configuration at Site A – USM main campus, reference to Res2Dinv software	97
Table 4.9	Errors occurred on testing the selected regression model for Wenner-Schlumberger at Site B – Sungai Batu, Pulau Pinang, reference to Res2Dinv software	102
Table 4.10	Errors occurred on testing the selected regression models for the three arrays at Site C – USM Engineering campus, reference to Res2Dinv software	104
Table 4.11	Errors occurred on testing the selected regression model for Wenner and Wenner-Schlumberger at Site D – Lembah Bujang, reference to Res2Dinv software	111
Table 4.12	Errors occurred on testing the selected regression model for Wenner-Schlumberger array at Site E – Ulu Slim, Perak, reference to Res2Dinv software	114

Table 4.13	Errors occurred on testing the regression model for Wenner-Schlumberger array at Site F – Aceh Besar Regency, reference to Res2Dinv software	117
Table 4.14	Errors occurred on testing the regression model for Wenner-Schlumberger array at Site G – Sabah, Borneo, reference to Res2Dinv software	118
Table 4.15	Errors occurred in testing the selected regression model for Wenner array at Site H – University of Lagos campus, Nigeria, reference to Res2Dinv software	120
Table 4.16	MLR models’ performance compared with SCLS and IGN techniques	123

## LIST OF FIGURES

		<b>Page</b>
Figure 2.1	Electric current, $I$ flowing through a cylinder of uniform material, with resistivity, $\rho$ , cross-sectional, $A$ and length, $L$ produces a potential difference, $V$ (Modified from Lowrie, 2007)	11
Figure 2.2	Current flow through an electrode (Modified from Lowrie, 2007)	12
Figure 2.3	Cross-section of current and equipotential lines produced between a current source and sink (Modified from Reynolds, 1997)	14
Figure 2.4	Four-point electrode configuration for resistivity measurement (Modified from Kearey et al., 2002)	15
Figure 2.5	Current and potential electrodes geometry for Wenner array (Modified from Telford et al., 1990)	17
Figure 2.6	Current and potential electrodes geometry for Wenner-Schlumberger array (Modified from Telford et al., 1990)	18
Figure 2.7	Current and potential electrodes geometry for Dipole-dipole array (Modified from Telford et al., 1990)	19
Figure 3.1	Research methodology flowchart	46
Figure 3.2	Data acquisition and pre-processing flowchart	50
Figure 3.3	Geology map of Penang Island (Modified from Pradhan & Lee, 2010)	52
Figure 3.4	Survey layout for calibration profiles at USM main campus	52
Figure 3.5	Flowchart of basic regression diagnostic checks, data filtering and model calibration for the research work	57
Figure 3.6	Flowchart of model validation work	61
Figure 3.7	Survey layout for validation profiles at USM main campus	63
Figure 3.8	Geology map of Penang Island showing Sungai Batu area (Modified from Pradhan & Lee, 2010)	64
Figure 3.9	Survey layout for validation profiles at Sungai Batu	64

Figure 3.10	Geology map of part of Malaysian Peninsula showing USM Engineering campus, Nibong Tebal (Modified from Ariffin et al., 2015)	65
Figure 3.11	Survey layout for validation profiles at USM Engineering campus	66
Figure 3.12	Geology map of Lembah Bujang (Modified from Jane, 1991)	67
Figure 3.13	Survey layout for validation profiles at Lembah Bujang	68
Figure 3.14	Geology map of Ulu Slim (Modified from Jane, 1991)	69
Figure 3.15	Survey layout for validation profiles at Ulu Slim	70
Figure 3.16	Geology map of Aceh Besar Regency Aceh Besar Regency, Sumatra (modified from Bennett et al., 1981)	71
Figure 3.17	Survey layout for validation profile at Pulo, Seulimeum, Aceh Besar	72
Figure 3.18	Geology map of Tongod, Sabah (modified from Ismail, 1994)	74
Figure 3.19	Survey layout for validation profile at Tongod, Sabah	74
Figure 3.20	Geology map of Lagos State (Modified from Iwugo et al., 2003)	76
Figure 3.21	Survey layout for validation profile at University of Lagos Nigeria	76
Figure 4.1	Linear regression basic assumptions check (a) normality using boxplots and (b) linearity using scatterplots of the original and transformed datasets	81
Figure 4.2	Regression basic assumptions checks (a) histograms (b) normal probability plots and (c) scatterplots of standardized residuals for both datasets	83
Figure 4.3	Significance of additional variables ( $x$ and/or $z$ ) in the models	94
Figure 4.4	True resistivity contour plots of line AWNL4 estimated using regression models, WN1-WN4 generated for Wenner array, reference to Res2Dinv software	98
Figure 4.5	True resistivity contour plots of line AWSL2 estimated using regression models WS1-WS4, for Wenner-Schlumberger array, reference to Res2Dinv software	100

Figure 4.6	True resistivity contour plots of line ADDL2 estimated using regression models, DD1-DD4 for Wenner-Schlumberger array, reference to Res2Dinv software	101
Figure 4.7	True resistivity contour plots of line BWSL1 estimated using regression model, WS3 for Wenner-Schlumberger array, reference to Res2Dinv software	103
Figure 4.8	True resistivity plots of lines (a) CWNL1 and (b) CWNL2 estimated using regression model, WN1 for Wenner array, reference to Res2Dinv software	106
Figure 4.9	True resistivity plots of lines (a) CWSL1 and (b) CWSL2 estimated using regression model, WS3 for Wenner-Schlumberger array, reference to Res2Dinv software	108
Figure 4.10	True resistivity plots of lines (a) CDDL1 and (b) CDDL2 estimated using regression model, DD4 for Dipole-dipole array, reference to Res2Dinv software	110
Figure 4.11	True resistivity plots of lines (a) DWNL1 and (b) DWNL2 estimated using regression model, WN1 for Wenner array, reference to Res2Dinv software	113
Figure 4.12	True resistivity contour plots of line DWSL1 estimated using regression model, WS3 for Wenner-Schlumberger array, reference to Res2Dinv software	114
Figure 4.13	True resistivity plots of lines (a) EWSL1 and (b) EWSL2 estimated using regression model, WS3 for Wenner-Schlumberger array, reference to Res2Dinv software	116
Figure 4.14	True resistivity contour plots of line FWSL1 estimated using regression model, WS3 for Wenner-Schlumberger array, reference to Res2Dinv software	118
Figure 4.15	True resistivity contour plots of line GWSL1 estimated using regression model, WS3 for Wenner-Schlumberger array, reference to Res2Dinv software	119
Figure 4.16	True resistivity contour plots of line HWNL1 estimated using regression model, WN1 for Wenner array, reference to Res2Dinv software	121
Figure 4.17	True resistivity estimation templet (a) blank (b) filled with apparent resistivity data	124
Figure 4.18	Estimated true resistivity data ready to be copied for post-processing	125



## LIST OF SYMBOLS

$a$	Electrodes spacing
$A$	Area of cross section
cm	centimetre
$E$	Electric field
$G$	Conductance
$I$	Current
$J$	Current density
$k$	Geometrical parameter
$L$	Length
m	Meter
$n$	Ratio of the spacing between C and P
P	Potential
$r$	Radius
R	Resistance
$R^2$	Coefficient of determination
$R^2_{adj}$	Adjusted coefficient of determination
S	Siemens
v	Volume
V	Voltage
$x$	Horizontal location
$z$	Depth
$\Delta$	Change
°	Degree
>	Greater than
$\geq$	Greater than or equal to
<	Less than
$\leq$	Less than or equal to
-	Minus
+	Plus
$\pm$	Plus or minus
$\beta_0$	Intercept
$\beta$	Slope
$\Omega\text{m}$	Ohm-metre
%	Percentage
$\pi$	Pi
$\rho$	Resistivity
$\varepsilon$	Standard error

## LIST OF ABBREVIATIONS

1-D	One-dimensional
2-D	Two-dimensional
3-D	Three-dimensional
ANN	Artificial neural network
calibr	calibration
CO <sub>2</sub>	Carbon dioxide
D.C.	Direct current
DD	Dipole-dipole array model
GPR	Ground penetrating radar
IGN	Incomplete Gauss Network
I.P.	Induced polarization
MLR	Multiple linear regression
multic	multicollinearity
NE	North-east
Res2Dinv	Resistivity two-dimensional inversion
RMS	Root-mean-square
SAS400	Signal averaging system 4000
SCLS	Standard constraint least-squares
SPSS	Statistical package for the social sciences
SW	South-west
USM	Universiti Sains Malaysia
valid	validation
VES	Vertical electrical sounding
VIF	Variance inflation factor
<i>wMAPE</i>	Weighted mean absolute percentage error
WN	Wenner array model
WS	Wenner-Schlumberger array model

**MODEL-MODEL REGRESI LINEAR BERGANDA BAGI  
PENGANGGARAN KEBERINTANGAN SEBENAR DARI PENGUKURAN  
KEBERINTANGAN KETARA**

**ABSTRAK**

Model-model regresi linear berganda (MLR) untuk anggaran pantas keberintangan sebenar subpermukaan daripada pengukuran keberintangan ketara telah dibangunkan dan dinilai dalam kajian ini. Tujuannya adalah untuk mengurangkan masa proses yang diperlukan untuk melaksanakan sonsang dengan algoritma konvensional. Susunatur yang dipertimbangkan adalah Wenner, Wenner-Schlumberger dan Dipole-dipole. Parameter yang dikaji ialah keberintangan ketara ( $\rho_a$ ), lokasi mendatar ( $x$ ) dan kedalaman ( $z$ ) sebagai pembolehubah bebas; sementara keberintangan sebenar ( $\rho_t$ ) ialah pembolehubah bersandar. Untuk keberintangan subpermukaan tidak linear, set data terlebih dahulu diubah kepada skala logaritma untuk memenuhi andaian regresi asas; kenormalan, kelinearan, kekolinearan berganda, imbangan paksi, “heteroscedasticity” dan “outliers”. Empat model, setiap satu untuk tiga jenis susun atur, kemudiannya dibangunkan berdasarkan hierarki hubungan linear berganda antara pembolehubah bersandar dan pembolehubah bebas. Pekali MLR yang terhasil digunakan bagi menganggar  $\rho_t$  untuk set data  $\rho_a$ ,  $x$  dan  $z$  yang berbeza untuk pengesahan. Ketepatan model dinilai menggunakan pekali penentuan ( $R^2$ ), pekali penentuan yang diselaraskan ( $R^2_{adj}$ ), ralat punca min kuasa dua ( $RMSE$ ) dan peratusan ralat min mutlak berpemberat ( $wMAPE$ ). Nilai kalibrasi model,  $R^2$  telah didapati sebagai 0.75-0.76 untuk model-model susunatur Wenner, 0.63-0.71 untuk model-model susunatur Wenner-Schlumberger dan 0.47-0.66 untuk model-model susunatur

Dipole-dipole. Begitu juga dengan *RMSE* dan *wMAPE* yang diperoleh untuk semua model yang dihasilkan adalah dalam julat 3-8 %. Satu model terbaik untuk setiap daripada tiga model dipilih berdasarkan penilaian ketepatan. Apabila dibandingkan dengan sonsangan kekangan piawai kuasa dua terkecil (SCLS) dan algoritma tidak lengkap Gauss-Newton (IGN), model-model MLR telah didapati berkurangan masa pemprosesan yang diperlukan sehingga 80-92 % untuk menjalankan sonsangan dengan algoritma SCLS. Akhir sekali, model terpilih telah digunakan untuk membangunkan satu templat untuk anggaran pantas keberintangan sebenar dalam platform Microsoft Excel. Ia dapat disimpulkan bahawa model-model MLR boleh menganggar  $\rho_t$  dengan pantas untuk pelbagai susunatur dengan tepat.

**MULTIPLE LINEAR REGRESSION MODELS FOR ESTIMATING TRUE  
SUBSURFACE RESISTIVITY FROM APPARENT RESISTIVITY  
MEASUREMENTS**

**ABSTRACT**

Multiple linear regression (MLR) models for rapid estimation of true subsurface resistivity from apparent resistivity measurements are developed and assessed in this study. The objective is to minimize the processing time required to carry out inversion with conventional algorithms. The arrays considered are Wenner, Wenner-Schlumberger and Dipole-dipole. The parameters investigated are apparent resistivity ( $\rho_a$ ), horizontal location ( $x$ ) and depth ( $z$ ) as independent variable; while true resistivity ( $\rho_t$ ) is dependent variable. To address the nonlinearity in subsurface resistivity distribution, the datasets were first transformed into logarithmic scale to satisfy the basic regression assumptions; normality, linearity, multicollinearity, axis balance, heteroscedasticity and outliers. Four models, each for the three array types, were developed based on hierarchical multiple linear relationships between the dependent variable and the independent variables. The generated MLR coefficients were used to estimate  $\rho_t$  for different  $\rho_a$ ,  $x$  and  $z$  datasets for validation. Accuracy of the models was assessed using coefficient of determination ( $R^2$ ), adjusted coefficient of determination ( $R^2_{adj}$ ), root-mean-square error ( $RMSE$ ) and weighted mean absolute percentage error ( $wMAPE$ ). The model calibration,  $R^2$  values were obtained as 0.75-0.76 for Wenner array models, 0.63-0.71 for Wenner-Schlumberger array models and 0.47-0.66 for Dipole-dipole array models. Similarly, the  $RMSE$  and  $wMAPE$  obtained for all the models developed were in the range of 3-8 %. One best model each for the

three arrays was thus selected based on the accuracy assessment. When compared with Standard Constraint Least-Squares (SCLS) inversion and Incomplete Gauss-Newton (IGN) algorithms, the MLR models have been found to reduce up to 80-92 % of the processing time required to carry out the inversion with the SCLS algorithm. Finally, the selected models were used to develop a template for fast estimation of the true resistivity on Microsoft Excel platform. It is concluded that the MLR models can rapidly estimate  $\rho_t$  for the various arrays accurately.

# CHAPTER 1

## INTRODUCTION

### 1.0 Background

In a general context, geophysics may be defined as a subject that applies physics principles to investigate the Earth, Moon and other planets (Telford et al., 1990). This is particularly achieved through conducting and interpreting measurements of the Earth's physical properties to ascertain its subsurface conditions to realize a desired goal (Kearey et al., 2002). Exploration geophysics, on the other hand, is concerned with investigating the Earth's crust and its near surface to achieve practical and economic objectives. It covers wide range of applications such as experiments to determine the thickness of overburden or sediments, study of shallow structures for exploring minerals, groundwater and other economic resources. In addition, it is concerned with surveys to locate narrow mine shafts and other forms of buried structures such as pipes, cables and cavities, or mapping of archaeological remains (Reynolds, 1997).

Detection of structures beneath the ground surface therefore depends upon those properties that distinguish them from the surrounding media. Different methods may thus be applied to wide range of investigations depending on their suitability to resolve the target structure in relation to its surrounding environment. For example, seismic method takes the advantage of contrast in velocity of acoustic waves as they propagate through the subsurface to distinguish between rocks and soils of varied materials (Moorkamp et al., 2013). Magnetic method is efficient only when magnetic susceptibility contrasts can be used to differentiate underground materials (Dalan et

al., 2017; Davey, 2017). Same goes to gravity when variations in density distribution are used to identify targets of interest (Saad et al., 2014; Wada et al., 2017). Ground Penetrating Radar (GPR) is also another powerful tool used for very shallow studies, particularly when subsurface structures are distinguishable by their conductivity or reflectivity to radar pulses (Ebrahimi et al., 2017).

In the same manner, electrical resistivity method uses contrast in resistivity distribution to distinguish between subsurface materials (Yao et al., 2017). The method injects current into the ground using two current electrodes. Electric potential can then be measured using another set of electrodes in the neighbourhood of the current flow. Since the magnitude of current applied is usually known, it is therefore possible to calculate the effective underground resistivity. This particularly makes resistivity (theoretically) superior to all other electrical methods, as quantitative results are obtained through the application of a controlled current source of specific dimensions (Telford et al., 1990). However, despite the advantages, the potentialities of resistivity are still not fully maximized, probably due to its high sensitivity to minor variations in subsurface conductivity.

Resistivity method has been applied to solve many practical problems such as in engineering and environment (Bery & Saad, 2012b; Abdulrahman et al., 2013; Syukri et al., 2013), hydrological investigations (Massoud et al., 2015), exploration of mineral deposits (Chambers et al., 2012), detection of buried metallic objects and cavities (Vachirastienchai & Siripunvaraporn, 2013a), and more recently in shallow archaeological investigations (Saad et al., 2014). It has equally been proved useful in hydrocarbon exploration and forensic studies (Reynolds, 1997); and in regional geological investigations (Ali et al., 2013) covering areas of hundreds of square kilometres or even more (Reynolds, 1997). This is achievable considering how the

method has progressively developed especially in data acquisition and processing techniques (Rucker et al., 2012; Loke et al., 2015; Anders et al., 2016; Ingeman-Nielsen et al., 2016). Resistivity and electromagnetic methods are likely be the most applied among the other geophysical methods (Reynolds, 1997).

Just like in the case of most other geophysical methods, apparent resistivity data acquired on site are not normally interpreted directly. Inversion is required to build true subsurface resistivity model from the measured apparent resistivity data (Narayan et al., 1999a; Loke et al., 2015a). Inversion algorithms based on different theoretical frameworks have been developed and are still being upgraded to accomplish this task (Kiflu et al., 2016). In conjunction with recommendations and gaps in literature, new multiple linear regression models are developed and assessed in this study, based on three physical parameters derived from subsurface apparent resistivity measurements.

## **1.1 Problem statements**

Resistivity method is one of the few geophysical exploration tools applied to solve many exploration related problems such as groundwater (Saad et al., 2012a), mineral prospecting (Song et al., 2017) and investigating engineering construction sites (Dahlin at al., 2007; Bery and Saad, 2012b). However, resistivity data acquired on site are apparent (not true) and cannot therefore be used directly to characterize the subsurface materials (De Donno and Cardarelli, 2017). Inverse modelling of such apparent resistivity measurements is necessary if the true subsurface resistivity model is to be actualized.

Many resistivity inversion techniques have been developed for many years and still being enhanced to curtail the problems associated with its speed and efficacy (Bergmann et al., 2014). The least squares optimization-based techniques are the most conventional but are particularly susceptible to problems such as emergence of false anomalies at intermediate and later iterations, consume a lot of time for the iterative computations to converge at minimum data misfit (VachiratiENCHAI and Siripunvaraporn, 2013) and difficulties in dealing with nonlinear relationships among the modelling parameters (Singh et al., 2010). Even more recently, Loke et al. (2015) demonstrated that variability in the true subsurface resistivity as explained by the apparent resistivity measurement parameters is not completely known. Thus, an additional independent variable is entered into inversion routine without adequate knowledge on how much it can contribute to the overall inversion accuracy.

To minimize the processing time required for inversion with conventional techniques, this research is focused to develop linear regression models for estimating true subsurface resistivity, based on measured apparent resistivity data. The models are also compared with results from Res2Dinv software for validation.

## **1.2 Research objectives**

The main aim of this research is to develop multiple linear regression models for rapidly estimating true subsurface resistivity from apparent resistivity measurements. The research has the following specific objectives which are;

- i. To develop and assess linear regression models for estimating true subsurface resistivity from apparent resistivity data

- ii. To evaluate the contribution of apparent resistivity to the variability in true subsurface resistivity when other variables are not involved
- iii. To assess the efficacy of the linear regression models to reduce processing time as compared with other established techniques available in Res2Dinv software
- iv. To develop a template for fast estimation of the true resistivity on Microsoft Excel platform, using the selected models for each array

### **1.3 Scope of the study**

In this study, multiple linear regression models for estimating true subsurface resistivity from apparent resistivity measurements have been developed and assessed. Only three arrays configuration; Wenner, Wenner-Schlumberger and Dipole-dipole were considered, for they are the most commonly used of the arrays configuration available (Telford et al., 1990). The parameters used in developing the models were apparent resistivity ( $\rho_a$ ), horizontal location ( $x$ ) and depth ( $z$ ) of measurements as the independent variables, with the true resistivity ( $\rho_t$ ) being the dependent variable. The independent variables were not measured directly but are spontaneously computed from combinations of several other measurable parameters as measurements are being carried out and can thus provide adequate representation of the entire survey measurements. They are equally the end result of any 2-D resistivity measurement, and they together allow for the plotting the apparent resistivity pseudo section. Furthermore, the calibration data was acquired at Universiti Sains Malaysia, Pulau Pinang, Malaysia. The area is composed of residual

soil of uniform composition, making it suitable for the purpose of this study. The motivation to cautiously select a suitable area as a source of good data for the modelling cannot be overemphasized. The validation data was acquired at eight (8) arbitrary sites in various parts of Asia as well as in West Africa. This was done to ascertain the robustness of the models for accurate true resistivity estimation.

#### **1.4 Research significance and novelty**

This research work seeks to develop linear regression models for estimating true subsurface resistivity from apparent resistivity measurements obtained using Wenner, Wenner-Schlumberger and Dipole-dipole arrays. The models produced reasonable true resistivity estimates when compared side by side with results obtained from Res2Dinv software, at much lesser time. The research has also managed to evaluate the contribution of apparent resistivity to the variability in true subsurface resistivity when other variables are not involved.

This research also owes its originality to the fact that it is the first of its kind to provide alternative means for rapidly estimating true subsurface resistivity using a simple template constructed from linear regression coefficients derived from apparent resistivity field measurements, without recourse to complex inversion algorithms. It is also the first to quantify the contributions of measured apparent resistivity to variability in true resistivity by empirical means. The same method can be adopted to examine other arrays and parameters that have not been investigated in this study.

## **1.5 Thesis layout**

This thesis is itemized into five distinct chapters. Chapter one is the introductory chapter, in which the background to the study is first presented. The next section discussed the problem statement which is a consequence of the knowledge gap discovered from literature. To address the problems, specific objectives are thus outlined in the subsequent section. Lastly, significance of the research is discussed, and emphasis is made on its novel contributions to knowledge.

Chapter two presents review of related literature, particularly on resistivity inversion. The chapter discussed and summarized previous research works aimed at addressing inversion related problems. In the process gaps were identified, which formed the basis for this study.

Chapter three discussed the resistivity method generally, with emphasis on its fundamental theoretical framework. Data acquisition methods for the arrays under investigation are also highlighted. Concept of multiple linear regression is then discussed, both in theory and application. The methodology designed to achieve the objectives of this research is explained and illustrated. Emphasis is also made on data processing, modelling and validation procedures. Finally, geology of the study is also described.

Chapter four presents result of the research. It demonstrates the performance of data transformation to achieving linearity and normality in resistivity datasets. It also presents the resistivity models developed and showcases their robustness and efficacy to estimating the true resistivity. This is evident when apparent resistivity data along eighteen (18) at eight (8) arbitrary sites in various parts of Asia and in West Africa were acquired and processed using both the linear regression models of

this study and Res2Dinv software for comparison. The *RMSE* and *wMAPE* of the estimates computed show that the errors occurred were generally less than 13 %, which is far below the 26 % signifying poor convergence for resistivity inversion which becomes high when it reaches 40 % (Wilkinson et al., 2012). The percentage contributions of apparent resistivity to the variations in true resistivity have also been quantified and presented in the chapter. Comparisons are also made between the three arrays investigated as well as with other established techniques. A template for fast estimation of the true resistivity has finally been developed and tested on Microsoft Excel platform.

Chapter five concludes the major findings of this study and provides recommendations for future research.

## CHAPTER 2

### LITERATURE REVIEW

#### 2.0 Introduction

This chapter presents review of previous work relevant to this study. Theoretical framework of resistivity method and arrays configuration are first discussed to provide general background and basic understanding for the research subject. A brief account of Res2Dinv software, as famous tool for resistivity data inversion, is also provided. Review of related literature is then presented to appraise the contributions made by previous researchers and to identify gap to be filled by the present study. Summary and comments are finally given with emphasis on the merits and demerits of the major techniques.

#### 2.1 Fundamentals of resistivity method

Resistivity method injects an artificially generated current into the ground, most commonly through point electrodes. Electric potential is then measured using pair of electrode near the current flow. It is therefore possible to calculate the underground effective or apparent resistivity since the magnitude of current applied is usually known. True resistivity estimated from the measurements is related to several other geological parameters or factors such as mineral content, porosity, pore fluid type and degree of saturation to identify geological features. It is important to note that resistivity of varied materials vary in a wider range depending on these factors. Metallic ores, for example, can have resistivity values of  $10^{-5}$   $\Omega\text{m}$  compared

to about  $10^8 \Omega\text{m}$  obtained in dry marble. Resistivity of most other common materials fall between these extreme values (Table 2.1). Resistivity survey therefore takes advantage of the large contrast to easily locate a low resistivity orebody in a high resistivity host rock (Telford et al., 1990).

Table 2.1: Resistivity of some common rocks and soil materials (Reynolds, 1997; Lowrie, 2007)

Material	Resistivity, $\rho$ ( $\Omega\text{m}$ )
Granite	$3 \times 10^2 - 10^6$
Granite (weathered)	$3 \times 10 - 5 \times 10^2$
Schist (calcareous and mica)	$20 - 10^4$
Quartzite	$10^3 - 10^5$
Basalt	$1 - 10^5$
Graphite	$10^{-4} - 10^{-2}$
Graphitic Schist	$10^{-1} - 50$
Sandstone	$1 - 7.4 \times 10^8$
Limestone	$10 - 10^7$
Clay	$1 - 10^2$
Alluvium	$1 - 10^3$
Consolidated shale	$20 - 2 \times 10^3$
Sand and gravel	$10 - 10^4$

The fundamental physics principle governing resistivity method is the one established by German scientist; Georg Simon Ohm in 1827, that electric current,  $I$  in a conducting medium is directly proportional to potential difference,  $V$  across the conductor. This is called Ohm's Law and expressed by Equation 2.1

$$V = IR \quad (2.1)$$

Where;

$R$  is resistance of medium (Ohm,  $\Omega$ ).

The reciprocal of resistance is conductance,  $G$  with unit as inverse Ohm ( $\Omega^{-1}$ ) or simply Siemens (S). It has been established from experiments that for a uniform material, its resistance is found to be directly proportional to its length,  $L$  and inversely proportional to an area of cross section,  $A$  (Figure 2.1). This can be expressed mathematically as Equation 2.2

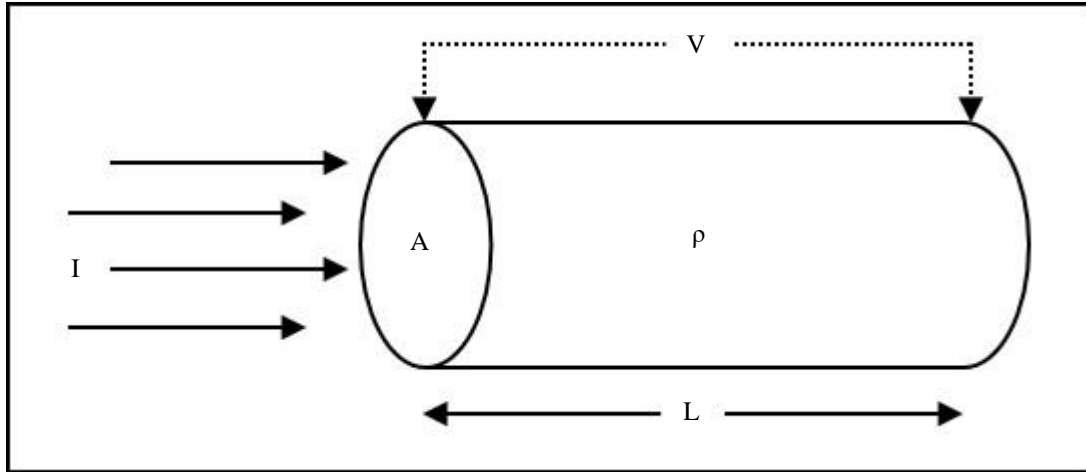


Figure 2.1: Electric current,  $I$  flowing through a cylinder of uniform material, with resistivity,  $\rho$ , cross-sectional,  $A$  and length,  $L$  produces a potential difference,  $V$  (Modified from Lowrie, 2007)

$$R = \rho \frac{L}{A} \quad (2.2)$$

Where;

$\rho$  is proportionality constant, known as resistivity of the material.

Resistivity is defined as the physical property of the material which dictates its ability to oppose the flow of electric current with the units  $\Omega\text{m}$ . Just like the resistance, reciprocal of resistivity is called conductivity,  $\sigma$  and expressed in  $\Omega^{-1}\cdot\text{m}^{-1}$  (Kearey et al., 2002).

Suppose that Equation 2.2 is substituted in Equation 2.1 and rearranged, Equation 2.3 will thus emerge

$$\frac{V}{L} = \rho \frac{I}{A} \quad (2.3)$$

The ratio of  $I/A$  in the right hand side of the Equation denotes the current density,  $J$  defined as current per unit area. The ratio,  $V/L$  in the left hand side also corresponds to electric field,  $E$ . Equation 2.3 can therefore be rewritten as Equation 2.4

$$E = \rho J \quad (2.4)$$

The form of equation expressed by Equation 2.4 is particularly useful for resistivity computations in resistivity survey, even though the physical quantities,  $V$  and  $I$  are still measured and recorded in the survey (Lowrie, 2007).

Suppose that current is supplied to the surface of a uniform half space via an electrode, the contact point serves as current source, from which the current radiates outward. The electric flux is parallel to the direction of flow of current and perpendicular to the equipotential surface (Figure 2.2).

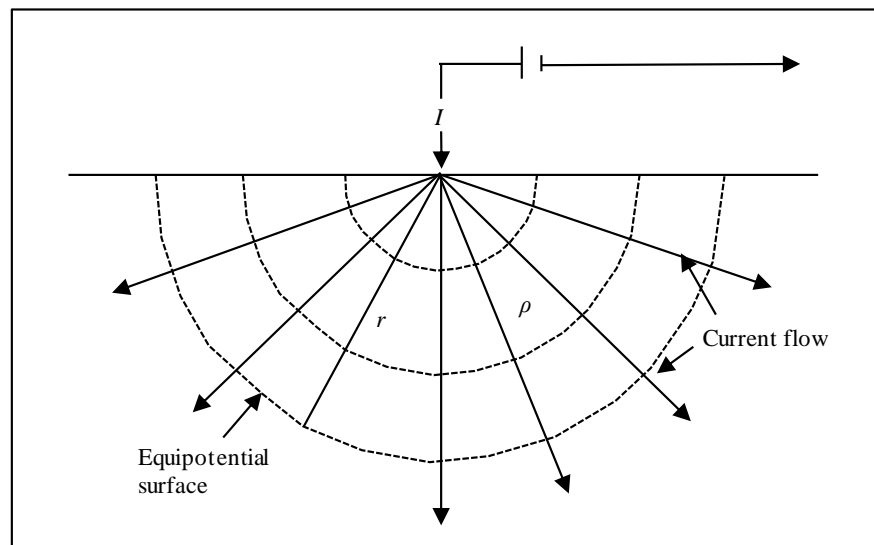


Figure 2.2: Current flow through an electrode (Modified from Lowrie, 2007)

Since current density,  $J$  is given by,  $I/A$  where  $A$  is defined as  $2\pi r^2$  for hemisphere of radius,  $r$ , the electric field,  $E$  at a distance,  $r$  from the electrode can be modified from Equation 2.4 as Equation 2.5

$$E = \rho J = \rho \frac{I}{2\pi r^2} \quad (2.5)$$

But, potential difference,  $\partial V$  across a hemispherical shell of thickness,  $\partial r$  is defined as  $-E\partial r$  or as expressed in Equation 2.6

$$\frac{\partial V}{\partial r} = -E = -\rho \frac{I}{2\pi r^2} \quad (2.6)$$

Thus, the potential difference,  $V$  at a distance,  $r$  from the current source (given by Equation 2.7) is obtained by integrating both sides of Equation 2.6

$$V = \rho \frac{I}{2\pi r} \quad (2.7)$$

Figure 2.7 shows that an electric flux around a source electrode which injects current into the ground is radially outwards, while in the case of a sink electrode through which current flows out of the subsurface, the flux is radially directed inwards. Hemispherical equipotential surfaces are thus observed beneath the source and sink electrodes if the two electrodes are regarded in isolation. Around the source, the potential is positive and thus decreases as distance increases. At sink however, the sign of  $I$  is negative and so,  $V$  is also negative. Increasing distance will therefore increase the magnitude of  $V$  since it becomes less negative (Equation 2.7). These hypothesis can therefore be used to compute potential difference between another pair of electrodes placed at specific distances from the current electrode (Lowrie, 2007).

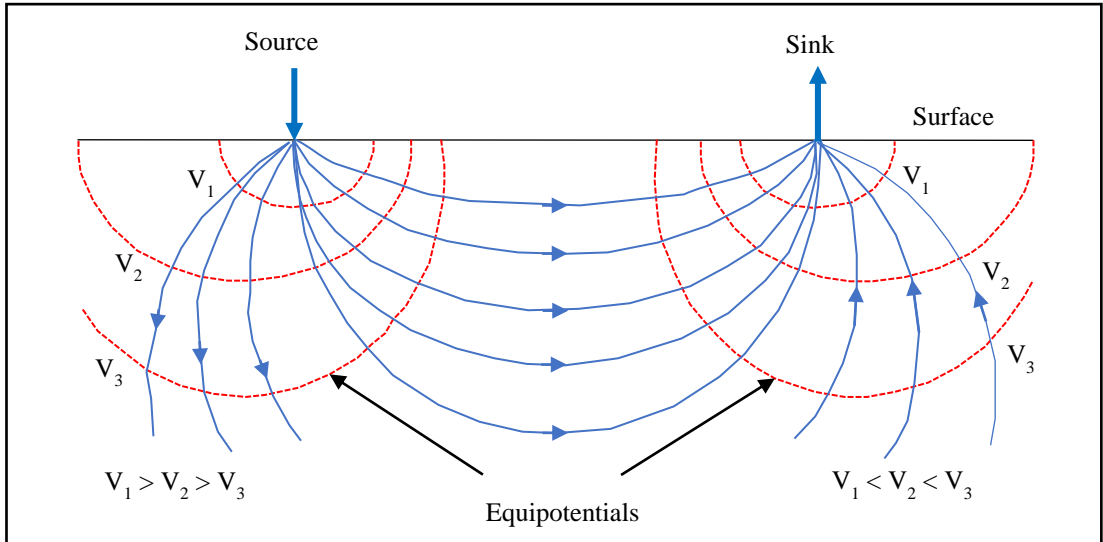


Figure 2.3: Cross-section of current and equipotential lines produced between a current source and sink (Modified from Reynolds, 1997)

## 2.2 Four electrodes method for measuring subsurface resistivity

Figure 2.4 depicts an arrangement consisting pairs of current and potential electrodes. The electrodes labelled A and B indicate the source and sink respectively. The potential due to the source, A at the detection electrode, C is  $+\rho I/2\pi r_1$ , whereas the potential due to sink, B at the same detection electrode, C is  $-\rho I/2\pi r_3$ . The resultant potential at C is therefore given as Equation 2.8

$$V_C = \frac{\rho I}{2\pi} \left( \frac{1}{r_1} - \frac{1}{r_3} \right) \quad (2.8)$$

Similarly, the effective potential due to the same source and sink at the detection electrode, D can be formulated as Equation 2.9

$$V_D = \frac{\rho I}{2\pi} \left( \frac{1}{r_2} - \frac{1}{r_4} \right) \quad (2.9)$$

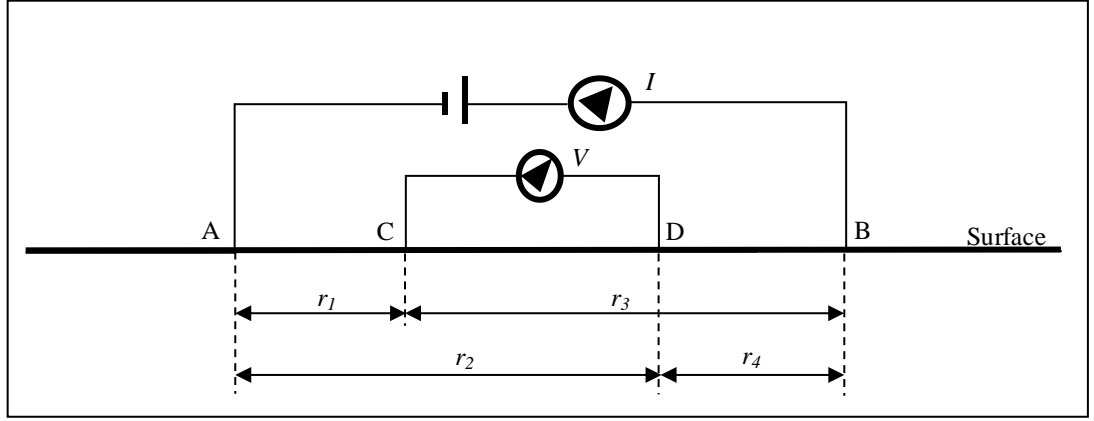


Figure 2.4: Four-point electrode configuration for resistivity measurement (Modified from Kearey et al., 2002)

The potential difference measured by a receiver connected across C and D is thus given as Equation 2.10

$$V = \frac{\rho I}{2\pi} \left\{ \left( \frac{1}{r_1} - \frac{1}{r_3} \right) - \left( \frac{1}{r_2} - \frac{1}{r_4} \right) \right\} \quad (2.10)$$

Since all parameters in Equation 2.10 can be measured directly on site apart from resistivity, the resistivity can thus be calculated when Equation 2.10 is rearranged to form Equation 2.11

$$\rho = 2\pi \frac{V}{I} \left( \frac{1}{r_1} - \frac{1}{r_2} - \frac{1}{r_3} + \frac{1}{r_4} \right)^{-1} \quad (2.11)$$

Equation 2.1 is inserted into Equation 2.11 to yield Equation 2.12 as

$$\rho = kR \quad (2.12)$$

where the geometrical parameter,  $k$  given by Equation 2.13 is defined for various arrays configuration. The apparent resistivity value will thus depend on the geometry of the electrode array used to measure it (Kearey et al., 2002).

$$k = 2\pi \left( \frac{1}{r_1} - \frac{1}{r_2} - \frac{1}{r_3} + \frac{1}{r_4} \right)^{-1} \quad (2.13)$$

The general resistivity formula is given by Equation 2.11, for certain special configurations of current and potential electrodes. Of the configurations available, the most commonly used are Wenner, Schlumberger and Dipole-dipole or Double-dipole (Telford et al., 1990). In this study however, a modified form of Schlumberger array, called Wenner-Schlumberger array is used together with Wenner and Dipole-dipole. This is because standard arrays are required to acquire data with a digital multi-electrode system with electrodes arranged at uniform spacing. In each of the configurations, all the four electrodes are collinear, but the major differences are in spacing and geometry.

### 2.2.1 Wenner array

Wenner array configuration applies all four the electrodes spaced uniformly in line, in such a way that both current and potential electrode pairs are having common mid-point (Figure 2.5). Therefore,  $r_1 = r_4 = a$  and  $r_2 = r_3 = 2a$  (Figure 2.4). Inserting the notation into Equation 2.13 will return,  $k = 2\pi a$ . The apparent resistivity in Equation 2.12 can now be rewritten as Equation 2.14 for Wenner array.

$$\rho = 2\pi a R \quad (2.14)$$

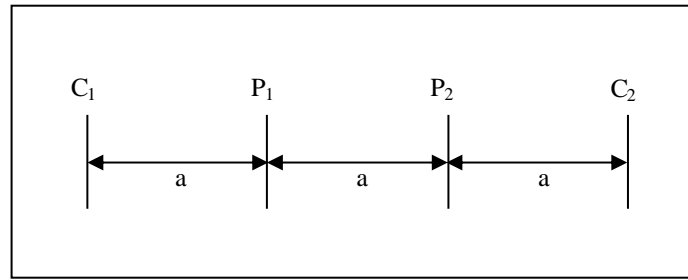


Figure 2.5: Current and potential electrodes geometry for Wenner array (Modified from Telford et al., 1990)

For vertical sounding work using Wenner spread, electrodes are extended about the mid-point by increasing the spacing,  $a$  in steps until a desired depth of investigation is reached, since array length is proportional to depth. In the case of lateral exploration however, spacing between the electrodes is kept constant, but all the four electrodes are shifted horizontally in line until the survey line is completed. For both cases, the apparent resistivity value measured is plotted against the spread centre, specified by horizontal location and depth. For two-dimensional survey, the two methods are combined in one system and measurements are carried out simultaneously (Milsom, 2003).

### 2.2.2 Wenner-Schlumberger array

As the name implies, Wenner-Schlumberger array arises from combination of Wenner and Schlumberger arrays to carryout survey works using the nowadays digital multi-electrode systems with electrodes arranged at constant spacing (Figure 2.6). A factor,  $n$  defines a ratio of the spacing between C<sub>1</sub> and P<sub>1</sub> (or C<sub>2</sub> and P<sub>2</sub>) to the distance between P<sub>1</sub> and P<sub>2</sub>. Similar analysis from Figure 2.4 provides,  $r_1 = r_4 = na$  and  $r_2 = r_3 = (na + a)$ . Substituting the notation into Equation 2.13 returns,

$k = \pi n(n+1)a$ . The apparent resistivity from Equation 2.12 can then be formulated as Equation 2.15 for Wenner-Schlumberger array (Loke, 2016).

$$\rho = \pi n(n+1)aR \quad (2.15)$$

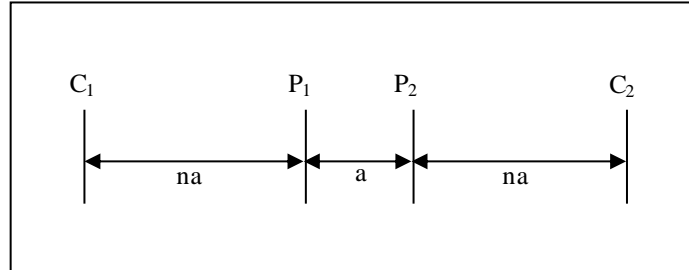


Figure 2.6: Current and potential electrodes geometry for Wenner-Schlumberger array (Modified from Telford et al., 1990)

### 2.2.3 Dipole-dipole array

Dipole-dipole array is arranged in such a way that the distance,  $a$  between both current ( $C_1$  and  $C_2$ ) and potential ( $P_1$  and  $P_2$ ) electrodes pairs is relatively small compared to the distance between the two pairs (or between  $C_1$  and  $P_1$ ). A factor,  $n$  which indicates integral multiple of the spacing,  $a$  is also defined for the array (Figure 2.7). Referring to Figure 2.4;  $r_1 = na$ ,  $r_2 = r_3 = (na + a)$  and  $r_4 = (na + 2a)$ , and substitute into Equation 2.13 will provide,  $k = \pi n(n+1)(n+2)a$ . The apparent resistivity formula for Dipole-dipole array can thus be written as Equation 2.16 (Lowrie, 2007).

$$\rho = \pi n(n+1)(n+2)aR \quad (2.16)$$

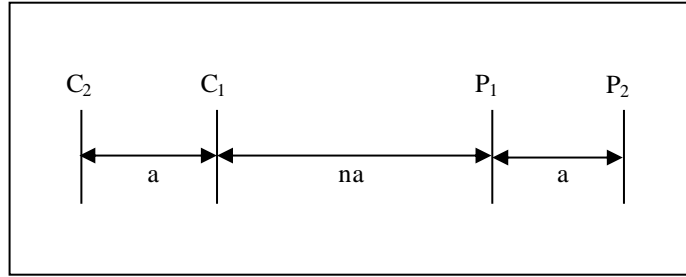


Figure 2.7: Current and potential electrodes geometry for Dipole-dipole array (Modified from Telford et al., 1990)

### 2.3 Inversion of resistivity data

The objective is this study to provide an alternative technique for processing apparent resistivity data to produce true resistivity, especially when processing time with conventional inversion algorithms, embedded in commercial software packages, is of primary concern. Some of the software packages available in the market are AIG EarthImager, ZondRes2d, Aarhusinv (Auken et al., 2015; Fiandaca et al., 2013), BERT (Rucker et al., 2006; Gunther et al., 2006) and Res2Dinv (Loke et al., 1996; Loke et al., 2003) among others. Of all these commercial software packages, Res2Dinv is the most prominent and widely accepted (Dahlin et al., 2007; Bery & Saad, 2012a; Saad et al., 2012a; Saad et al., 2012b; Abdulrahman et al., 2013; Syukri et al., 2013).

The software has inversion algorithms that seek to find a true resistivity model that gives a response similar to the actual measured apparent resistivity data. The model is an idealized mathematical representation of a section of the earth. The model is specified by a set of model parameters which are the physical quantities we want to estimate from the measured data. The model response is the synthetic data that can be calculated from the mathematical relationships defining the model for a given set of model parameters. The inversion algorithm essentially tries to determine

a model for the subsurface whose response agrees with the measured data subject to certain restrictions and within acceptable limits. An initial model is modified in an iterative manner so that the difference between the model response and the measured data values is reduced. The measure of this difference is given by root-mean-squared error (*RMSE*) or mean absolute percentage error (*MAPE*). In the cell-based method used by the Res2Dinv programs, the model parameters are the resistivity values of the model cells, while the data is the measured apparent resistivity values. The mathematical link between the model parameters and the model response for the 2-D resistivity models is provided by the finite-difference or finite-element methods (Loke, 2016).

## **2.4 Previous works**

Today, resistivity survey plays significant role in many large-scale sites characterization (Dahlin et al., 2007; Bery and Saad, 2012b), groundwater exploration (Saad et al., 2012a) and mineral prospecting (Saad et al., 2012c; Song et al., 2017). Unfortunately, the measured apparent resistivity data from such surveys cannot be used directly to describe the subsurface (De Donno and Cardarelli, 2017). There is, therefore, a need to develop resistivity models that can portray the true subsurface conditions based on the apparent resistivity measurements. The act of building such models is an inversion problem. Inverse modelling can be performed within certain allowable error limits (Narayan et al., 1999).

Resistivity inversion has received enormous attention from various researchers over the years. Investigations are still ongoing to further mitigate the problems associated its speed and efficacy. In this section, review of related previous

research works aimed to address these problems, is carried out. They are presented in accordance with the underlying theoretical frameworks upon which they were based. Prominent among such approaches are the least squares optimization, artificial neural network (ANN) and joint inversion. A few other approaches are also used but are generally less popular.

The readiness of apparent resistivity data inversion to build true subsurface resistivity model of a given 2-D geologic structure was assessed by Olayinka and Yaramanci (2000a) based on a smoothness constrained nonlinear least squares optimization technique using Wenner array. The assessment was carried out using synthetic apparent resistivity data derived from vertical fault, horizontal layered, up faulted basement block overlain by a conductive overburden and low resistivity infill over high resistivity basement models. The resistivity inversion models obtained were generally much sharper than the models built directly from the synthetic data over the vertical structure models. However, the inversion models had lower resistivity values than the lowest and higher values than the highest (extreme) values of the actual resistivity models. This has shown that only an approximate guide to the true geometry of a given formation can be achieved from the smooth inversion technique.

Olayinka and Yaramanci (2000b) again investigated the capability of a block inversion scheme to determining the geometry and true resistivity of subsurface structures and proposed a simple strategy for formulating the starting (initial) model. The strategy was based on plane layered Earth model to define layers and bodies of equal resistivity. The block inversion was also compared to the cell based smooth inversion scheme using synthetic and field examples. The results indicated that the smooth inversion can produce sharp images for resolving structural geometry but

could only provide rough estimates of true resistivity values due to the smearing effects. However, in the presence of sharp resistivity discontinuities, block inversion can resolve the subsurface geometry and resistivity more precisely.

Loke and Dahlin (2002) examined the strength and weakness of smoothness constrained least squares method for the inversion of 2-D and 3-D apparent resistivity datasets. In this approach, Jacobian matrix for a homogeneous earth model is utilized for the first iteration, and the matrix elements are subsequently adjusted in later iterations. Least squares equation is solved by applying the Gauss-Newton equation that recalculates the Jacobian matrix of partial derivatives. Time involved in the iterative computations of many dataset is minimized with the help of the quasi-Newton method. The authors further proposed an intermediate technique as a combination of Gauss-Newton and quasi-Newton methods, in which the partial derivatives are directly calculated for the first few iterations, and then updated by a quasi-Newton technique for subsequent iterations. Three inversion techniques were simultaneously tested with apparent resistivity data from synthetic model and test site. All the techniques performed roughly the same way for areas with moderate resistivity contrasts. However, with increasing resistivity contrasts, the quasi-Newton technique performed least. The Gauss-Newton was relatively better than combined method, but the combined method was considerably faster especially in dealing with many datasets.

Pain et al. (2002) developed a multidimensional resistivity inversion technique based on finite element, to represent electric potentials of each source problem and conductivities describing the model. Least squares approach was chosen to solve the inverse problem for the fact that quadratic terms to be optimized can be treated implicitly, making it possible to attain a near minimum after a single iteration.

Linear preconditioned conjugate gradients were used to solve both potential field source and least squares problems. Since the electrical inverse problem is ill-conditioned, model covariance matrices and data weighting were used to aid the inversion process to reach an appreciable result. The model covariance used permitted preferential model regularization in arbitrary directions and the application of spatially varying regularization. Two approaches for improving model resolution away from sources and receivers were demonstrated. The first approach investigated the practicality of applying smoothness constraints that depend on depth and change in direction. The second approach preferentially updates the data with additional weights containing extra information of poorly resolved areas. When tested with numerical and site examples, both methods improve the inversion model and aid the reconstruction algorithm to create model structure at depth.

In a similar attempt, Loke et al. (2003) reviewed the merits and demerits of smooth and blocky inversion techniques for 2-D resistivity inverse modelling, and summarized thus: the regularized (smooth) least squares optimization approach (with a cell based model) that seeks to minimize the squares sum of the spatial changes in the model resistivity is frequently applied for the inversion of resistivity data if structures with random resistivity distributions are to be sufficiently resolved. Hence, the inversion model produced has a smooth change in the resistivity values. However, for cases in which the subsurface constitute a few zones with roughly uniform internal resistivity distribution, but are separated by sharp boundaries, the smooth inversion technique tends to smear out the boundaries and produce too low or too high resistivity values. The blocky optimization method can then provide solutions to such problems by way of minimizing the sum of the absolute values of the spatial changes in the model resistivity. Based on a number of synthetic and field

tests on both approaches, it was concluded that the smooth inversion technique can perform better when applied in areas with gradual subsurface resistivity variations, while the blocky inversion approach produces better results for areas with sharp boundaries.

Pain et al. (2003) formulated a 3-D electrical imaging inversion method in anisotropic media with inhomogeneous conductivity distribution. In this method, the conductivity distribution is discretized using finite elements and is described by a second order tensor at each finite element node. The inversion approach was defined as a functional optimization in which data misfit and model covariance are measured by an error term using smoothness, anisotropy and deviation from a given starting model. The error function is minimized with the aid of an iterative preconditioned conjugate gradient solver as a Levenberg-Marquardt type method to bypass the actual computation of the Jacobian matrix. For each inversion, penalty parameters were chosen to gauge the level of model covariance information imposed. When tested with 2-D and 3-D synthetic model data, the inversion process was found to be highly nonlinear. The images obtained approximately reproduced the prominent features of the model. However, the magnitudes and directions of anisotropy anomalies were generally underestimated, with the inversion images blurred with sharp edges smoothed.

In another research, Loke and Lane (2004) modified the smoothness constrained least squares inversion technique for interpretation of resistivity data from land surveys to fit water bottom topography. This was done by using a distorted finite-element grid to estimate apparent resistivity values for inverse model. The first few rows of element grid were dedicated for modelling the water layer, and subsequent elements were used for the sub bottom resistivity distribution. The water